Quantum random walks with decoherent coins

Todd A. Brun,[1,*] H. A. Carteret,[2,†] and Andris Ambainis[1,‡]

[1]*Institute for Advanced Study, Einstein Drive, Princeton, New Jersey 08540*
[2]*Department of Combinatorics and Optimization, University of Waterloo, Waterloo, Ontario, Canada N2L 3G1*

The quantum random walk has been much studied recently, largely due to its highly nonclassical behavior. In this paper, we study one possible route to classical behavior for the discrete quantum walk on the line: the presence of decoherence in the quantum "coin" which drives the walk. We find exact analytical expressions for the time dependence of the first two moments of position, and show that in the long-time limit the variance grows linearly with time, unlike the unitary walk. We compare this to the results of direct numerical simulation, and see how the form of the position distribution changes from the unitary to the usual classical result as we increase the strength of the decoherence.

I. INTRODUCTION

In the classical discrete random walk, a particle is located at one of a set of definite positions (such as the set of integers on the line). In response to a random event—for example, the flipping of a coin—the particle moves either right or left. This process is iterated, and the motion of the particle is analyzed statistically. These systems provide good models for diffusion and other stochastic processes.

Considerable work has been done recently on quantum random walks, which are unitary (and hence reversible) systems designed as analogues to the usual classical case. There are two general approaches to the problem: *continuous* [1–3] and *discrete* [4–22] unitary walks. This paper is exclusively concerned with the discrete walk. In this discrete case, we introduce an extra "coin" degree of freedom (usually a single quantum bit) into the system. Just as in the classical random walk, the outcome of a "coin flip" determines which way the particle moves; but in the quantum case, both the "flip" of the coin and the conditional motion of the particle are unitary transformations. Different possible classical paths can interfere with each other.

In this paper we look at quantum walks on the infinite line. The particle is initially at position $x=0$ and is free to travel off to infinity in either direction. We will look at both the probability distribution in $p(x,t)=\langle x|\rho_t|x\rangle$, and at the long-time behavior of the moments $\langle\hat{x}\rangle$ and $\langle\hat{x}^2\rangle-\langle\hat{x}\rangle^2$ as functions of t.

For a classical random walk, $p(x,t)$ has the form of a binomial distribution, with a width which spreads like $\sqrt{t}$; the variance $\overline{x^2}-\overline{x}^2$ grows linearly with time. The variance in the quantum walk, by contrast, grows *quadratically* with time; and the distribution $p(x,t)$ has a complicated, oscillatory form. Both of these are effects of interference between the possible paths of the particle.

It should be possible to recover the classical behavior as some kind of limit of the quantum system. There are two obvious ways to regain the classical result. If the quantum "coin" is measured at every step, then the record of the measurement outcomes singles out a particular classical path. By averaging over all possible measurement records, one recovers the usual classical behavior [11].

Alternatively, rather than reusing the same coin every time, one could replace it with a *new* quantum coin for each flip. After a time t one would have accumulated t coins, all of them entangled with the position of the particle. By measuring them, one could reconstruct an unique classical path; averaging over the outcomes would once again produce the classical result.

These two approaches, which are equivalent in the classical limit, give two different routes from quantum to classical [23]. We might increase the number of coins used to generate the walk, cycling among M different coins, in the limit using a new coin at each step. Or we might *weakly* measure the coin after each step, reaching the classical limit with strong, projective measurements. This is equivalent to having a coin which is subject to *decoherence*.

In another paper [24] we have considered the quantum random walk with multiple coins. In this case, the quantum behavior remains qualitatively unchanged until we reach the limit of a new coin for each step, at which point classical behavior is recovered.

In this paper, we consider the quantum random walk with a single coin subject to decoherence. We will see that in this case, the behavior is qualitatively quite different from the unitary quantum random walk. The usual classical solution is recovered in the limit where the coin decoheres completely every step; but even with weaker decoherence, the variance of the position distribution grows linearly with time, rather than quadratically (as in the unitary case).

In Sec. II we present an analytical result for the moments of the decoherent walk, and compare them to the results from direct numerical simulations. In Sec. III, we see how the probability distribution $p(x,t)$ changes as we introduce decoherence. Finally, in Sec. IV we summarize our results and state conclusions.

---

*Electronic address: tbrun@ias.edu
†Electronic address: hcartere@cacr.math.uwaterloo.ca
‡Electronic address: ambainis@ias.edu

II. MOMENTS OF THE DECOHERENT WALK

A. The unitary walk on the line

Let us now consider a fairly general quantum random walk on the line. The particle degree of freedom has a basis of position eigenstates $\{|x\rangle\}$, where x can be any integer. The position operator is $\hat{x}$, and $\hat{x}|x\rangle = x|x\rangle$. We will assume that the particle begins the walk at the origin, in state $|0\rangle$. The walk is driven by a separate "coin" degree of freedom: a D-dimensional system with an initial-state $|\Phi_0\rangle$. Let $\hat{\mathcal{P}}_R, \hat{\mathcal{P}}_L$ be two orthogonal projectors on the Hilbert space of the "coin," such that $\hat{\mathcal{P}}_R + \hat{\mathcal{P}}_L = \hat{I}$. These represent the two possible outcomes of the coin flip: heads or tails, right or left. We also define a unitary transformation $\hat{U}$ that "flips" the coin by rotating a coin showing heads or tails into a superposition of the two. One step of the quantum random walk is given by the unitary operator

$$\hat{E} \equiv (\hat{S} \otimes \hat{\mathcal{P}}_R + \hat{S}^\dagger \otimes \hat{\mathcal{P}}_L)(\hat{I} \otimes \hat{U}), \qquad (2.1)$$

where $\hat{S}, \hat{S}^\dagger$ are unitary shift operators on the particle position:

$$\hat{S}|x\rangle = |x+1\rangle, \quad \hat{S}^\dagger|x\rangle = |x-1\rangle. \qquad (2.2)$$

The full initial state of the system (particle and "coin") is

$$|\Psi_0\rangle = |0\rangle \otimes |\Phi_0\rangle. \qquad (2.3)$$

We can identify the eigenvectors $|k\rangle$ of $\hat{S}, \hat{S}^\dagger$,

$$|k\rangle = \sum_x e^{ikx}|x\rangle, \qquad (2.4)$$

with eigenvalues

$$\hat{S}|k\rangle = e^{-ik}|k\rangle,$$

$$\hat{S}^\dagger|k\rangle = e^{+ik}|k\rangle. \qquad (2.5)$$

The inverse transformation is

$$|x\rangle = \int_{-\pi}^{\pi} \frac{dk}{2\pi} e^{-ikx}|k\rangle. \qquad (2.6)$$

In particular, the initial state of the particle is

$$|0\rangle = \int_{-\pi}^{\pi} \frac{dk}{2\pi}|k\rangle. \qquad (2.7)$$

These state vectors $|k\rangle$ are not renormalizable, but if used with caution they greatly simplify the calculations. In the k basis, the evolution operator becomes

$$\hat{E}(|k\rangle \otimes |\Phi\rangle) = |k\rangle \otimes (e^{-ik}\hat{\mathcal{P}}_R + e^{ik}\hat{\mathcal{P}}_L)\hat{U}|\Phi\rangle \equiv |k\rangle \otimes \hat{U}_k|\Phi\rangle, \qquad (2.8)$$

where $\hat{U}_k$ is also a unitary operator.

The usual case considered in the literature has taken the coin to be a simple two-level system, and the "flip" operator $\hat{U}$ to be the usual Hadamard transformation $\hat{H}$:

$$\hat{H}|R\rangle = \frac{1}{\sqrt{2}}(|R\rangle + |L\rangle),$$

$$\hat{H}|L\rangle = \frac{1}{\sqrt{2}}(|R\rangle - |L\rangle). \qquad (2.9)$$

The projectors are $\hat{\mathcal{P}}_R = |R\rangle\langle R|$, $\hat{\mathcal{P}}_L = |L\rangle\langle L|$. The walk on the line in this case has been exactly solved by Nayak and Vishwanath [6].

For the present, we will continue without assuming a particular form for $\hat{U}$, $\hat{\mathcal{P}}_R$, or $\hat{\mathcal{P}}_L$. Later we will specialize to make comparison to numerical simulations.

B. Decoherence

We now generalize to allow for decoherence. Suppose that before each unitary "flip" of the coin, a completely positive map is performed on the coin (note, not on both the coin and the particle). This map is given by a set of operators $\{\hat{A}_n\}$ on the coin degree of freedom which satisfy

$$\sum_n \hat{A}_n^\dagger \hat{A}_n = \hat{I}. \qquad (2.10)$$

A density operator χ for the coin degree of freedom is transformed

$$\chi \rightarrow \chi' = \sum_n \hat{A}_n \chi \hat{A}_n^\dagger. \qquad (2.11)$$

If we apply this to a general density operator for the joint particle or coin system

$$\rho = \int \frac{dk}{2\pi} \int \frac{dk'}{2\pi}|k\rangle\langle k'| \otimes \chi_{kk'}, \qquad (2.12)$$

then after one step the state becomes

$$\rho \rightarrow \rho' = \int \frac{dk}{2\pi} \int \frac{dk'}{2\pi}|k\rangle\langle k'| \otimes \sum_n \hat{U}_k \hat{A}_n \chi_{kk'} \hat{A}_n^\dagger \hat{U}_{k'}^\dagger. \qquad (2.13)$$

The initial state is

$$\rho_0 = \int \frac{dk}{2\pi} \int \frac{dk'}{2\pi}|k\rangle\langle k'| \otimes |\Phi_0\rangle\langle\Phi_0|. \qquad (2.14)$$

Let the quantum random walk proceed for t steps. Then the state evolves to

$$\rho_t = \int \frac{dk}{2\pi} \int \frac{dk'}{2\pi}|k\rangle\langle k'| \otimes \sum_{n_1,\ldots,n_t} \hat{U}_k \hat{A}_{n_t} \cdots \hat{U}_k \hat{A}_{n_1}|\Phi_0\rangle$$

$$\times \langle\Phi_0|\hat{A}_{n_1}^\dagger \hat{U}_{k'}^\dagger \cdots \hat{A}_{n_t}^\dagger \hat{U}_{k'}^\dagger. \qquad (2.15)$$

We define the *superoperator* $\mathcal{L}_{kk'}$ on the coin degree of freedom

$$\int \frac{dk}{2\pi} \int \frac{dk'}{2\pi} |k\rangle\langle k'| \otimes \sum_n \hat{U}_k \hat{A}_n \chi_{kk'} \hat{A}_n^\dagger \hat{U}_{k'}^\dagger,$$

$$\equiv \int \frac{dk}{2\pi} \int \frac{dk'}{2\pi} |k\rangle\langle k'| \otimes \mathcal{L}_{kk'} \chi_{kk'}. \quad (2.16)$$

In terms of the superoperator,

$$\rho_t = \int \frac{dk}{2\pi} \int \frac{dk'}{2\pi} |k\rangle\langle k'| \otimes \mathcal{L}_{kk'}^t |\Phi_0\rangle\langle\Phi_0|. \quad (2.17)$$

Note that for $k=k'$ this superoperator preserves the trace. This implies that

$$\mathrm{Tr}\{\mathcal{L}_{kk}^n \hat{O}\} = \mathrm{Tr}\{\hat{O}\}, \quad (2.18)$$

for any operator $\hat{O}$. This identity will prove useful later.

The probability to reach a point x at time t is

$$p(x,t) = \mathrm{Tr}\{|x\rangle\langle x| \otimes \hat{I}\rho_t\} = \frac{1}{(2\pi)^2}\int dk \int dk' \langle k|x\rangle$$

$$\times \langle x|k'\rangle \mathrm{Tr}\{\mathcal{L}_{kk'}^t |\Phi_0\rangle\langle\Phi_0|\}$$

$$= \frac{1}{(2\pi)^2}\int dk \int dk' e^{-ix(k-k')} \mathrm{Tr}\{\mathcal{L}_{kk'}^t |\Phi_0\rangle\langle\Phi_0|\}.$$

$$(2.19)$$

C. Moments of position

Equation (2.19) for $p(x,t)$ will be difficult to evaluate, in general. However, we can get considerably further by restricting our interest to the *moments* of this distribution.

$$\langle \hat{x}^m \rangle_t = \sum_x x^m p(x,t)$$

$$= \sum_x x^m \int \frac{dk}{2\pi} \int \frac{dk'}{2\pi} e^{-ix(k-k')} \mathrm{Tr}\{\mathcal{L}_{kk'}^t |\Phi_0\rangle\langle\Phi_0|\}. \quad (2.20)$$

We can then invert the order of operations and do the x sum first. This sum can be exactly carried out in terms of derivatives of the δ function:

$$\frac{1}{2\pi}\sum_x x^m e^{-ix(k-k')} = (-i)^m \delta^{(m)}(k-k'). \quad (2.21)$$

Inserting this result back into our expression for $\langle \hat{x}^m \rangle_t$ yields

$$\langle \hat{x}^m \rangle_t = \frac{(-i)^m}{2\pi}\int dk \int dk' \delta^{(m)}(k-k') \mathrm{Tr}\{\mathcal{L}_{kk'}^t |\Phi_0\rangle\langle\Phi_0|\}. \quad (2.22)$$

We can then integrate this by parts.

In carrying out this integration by parts, we will need

$$\frac{d}{dk}\mathrm{Tr}\{\mathcal{L}_{kk'}\hat{O}\} = \sum_n \mathrm{Tr}\{(d\hat{U}_k/dk)\hat{A}_n\hat{O}\hat{A}_n^\dagger\hat{U}_{k'}^\dagger\}, \quad (2.23)$$

where

$$\frac{d\hat{U}_k}{dk} = -i(\hat{\mathcal{P}}_0 - \hat{\mathcal{P}}_1)\hat{U}_k \equiv -i\hat{Z}\hat{U}_k,$$

$$\frac{d\hat{U}_k^\dagger}{dk} = i\hat{U}_k^\dagger(\hat{\mathcal{P}}_0 - \hat{\mathcal{P}}_1) \equiv i\hat{U}_k^\dagger\hat{Z},$$

$$\hat{Z} = \hat{\mathcal{P}}_R - \hat{\mathcal{P}}_L = \hat{I} - 2\hat{\mathcal{P}}_L. \quad (2.24)$$

Substituting this back into Eq. (2.23) we get

$$\frac{d}{dk}\mathrm{Tr}\{\mathcal{L}_{kk'}\hat{O}\} = -i\mathrm{Tr}\{\hat{Z}\mathcal{L}_{kk'}\hat{O}\} = -i\mathrm{Tr}\{(\mathcal{L}_{kk'}\hat{O})\hat{Z}\}$$

$$= -\frac{d}{dk'}\mathrm{Tr}\{\mathcal{L}_{kk'}\hat{O}\}. \quad (2.25)$$

Making use of Eqs. (2.18) and (2.25), when we carry out the integration by parts for the first moment we get

$$\langle \hat{x} \rangle_t = -\frac{1}{2\pi}\sum_{j=1}^t \int dk \mathrm{Tr}\{\hat{Z}\mathcal{L}_{kk}^j |\Phi_0\rangle\langle\Phi_0|\}. \quad (2.26)$$

We can simplify our notation slightly by defining

$$\mathcal{L}_k \equiv \mathcal{L}_{kk}. \quad (2.27)$$

We can carry out a similar integration by parts to get the second moment:

$$\langle \hat{x}^2 \rangle_t = -\frac{1}{2\pi}\int dk \left[\sum_{j=1}^t \sum_{j'=1}^j \mathrm{Tr}\{\hat{Z}\mathcal{L}_k^{j-j'}(\hat{Z}\mathcal{L}_k^{j'} |\Phi_0\rangle\langle\Phi_0|)\} \right.$$

$$\left. + \sum_{j=1}^t \sum_{j'=1}^{j-1} \mathrm{Tr}\{\hat{Z}\mathcal{L}_k^{j-j'}[(\mathcal{L}_k^{j'} |\Phi_0\rangle\langle\Phi_0|)\hat{Z}]\} \right]. \quad (2.28)$$

Note that this form is rather similar to that for a correlation function.

For the unitary walk [23,24], we were able to separate the expressions for the moments into oscillatory and nonoscillatory terms, and consider only the nonoscillatory terms for the long-time limit. In the present case, this will not work; because of the presence of decoherence, the oscillations are damped. However, the long-time limit still simplifies in another way. If we think of $\mathcal{L}_k$ as a linear transformation, all its eigenvalues must clearly obey $|\lambda| \leq 1$ in order for it to be completely positive. In finding the long-time limit, we need
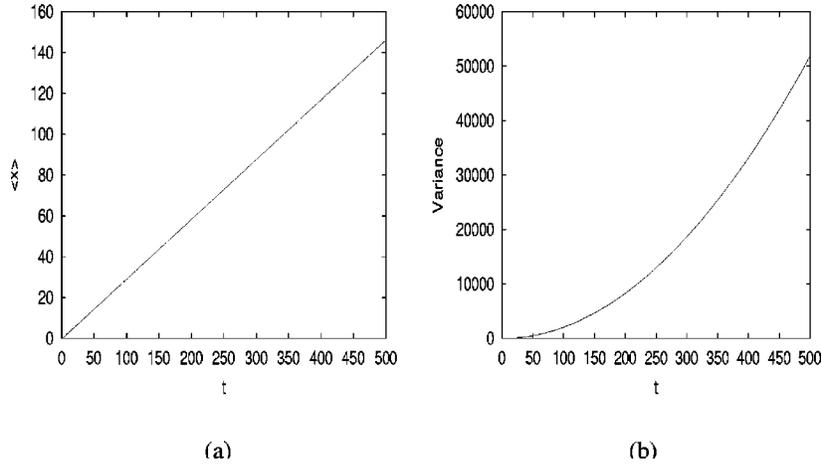
FIG. 1. The (a) expectation $\langle \hat{x} \rangle$, and (b) variance $\langle \hat{x}^2 \rangle - \langle \hat{x} \rangle^2$, for the Hadamard walk on the line without decoherence. The coin begins in state $|R\rangle$. Note that the first moment exhibits a linear drift with time, which seems to reflect a peculiar ''memory'' for the initial state; a system starting with the coin in state $|L\rangle$ would drift symmetrically in the other direction. The variance grows quadratically in time, in contrast to the linear growth in the classical random walk. Note that if viewed at a finer scale, both of these curves would exhibit oscillations about the simple power-law behavior.

pick out only those components of the expressions (2.26) and (2.28) which do not die away at large t.

D. The Hadamard walk with decoherence

To get any further than this, we need to specialize to a particular model. Let's choose the standard two-dimensional ''coin'' and the Hadamard walk as described above. This makes our operator $\hat{U}_k$,

$$\hat{U}_k = \frac{1}{\sqrt{2}} \begin{pmatrix} e^{-ik} & e^{-ik} \\ e^{ik} & -e^{ik} \end{pmatrix}. \tag{2.29}$$

We need also to pick a particular form for the decoherence. I will choose the decoherence produced by the three operators

$$\hat{A}_0 = \sqrt{p}|R\rangle\langle R|,$$

$$\hat{A}_1 = \sqrt{p}|L\rangle\langle L|,$$

$$\hat{A}_2 = \sqrt{1-p}\,\hat{I}. \tag{2.30}$$

This resembles a coin which has a probability p per step of being measured; however, this is equivalent to a large class of other decoherence models, such as *pure dephasing*,

$$\hat{A}_0' = \frac{1}{\sqrt{2}}(e^{i\theta}|R\rangle\langle R| + e^{-i\theta}|L\rangle\langle L|),$$

$$\hat{A}_1' = \frac{1}{\sqrt{2}}(e^{-i\theta}|R\rangle\langle R| + e^{i\theta}|L\rangle\langle L|), \tag{2.31}$$

or *weak measurement*,

$$\hat{A}_0'' = \sqrt{q}|R\rangle\langle R| + \sqrt{1-q}|L\rangle\langle L|,$$

$$\hat{A}_1'' = \sqrt{1-q}|R\rangle\langle R| + \sqrt{q}|L\rangle\langle L|. \tag{2.32}$$

All three of these decoherence processes represent the same completely positive map on the density matrix; one can transform from one to the other by invoking the relationships between the parameters,

$$1 - p = \cos 2\theta = 2\sqrt{q(1-q)}. \tag{2.33}$$

We will generally use the first in our derivations, for simplicity; but the second is more convenient for numerical calculations. Note that this equivalence applies to the *average* behavior over all outcomes; for a single sequence of outcomes, the conditional dynamics of these three decoherence (or weak measurement) models can look quite different.

In the absence of decoherence, the Hadamard walk exhibits a linear drift in $\langle \hat{x} \rangle$ and a quadratic growth in the variance $\langle \hat{x}^2 \rangle - \langle \hat{x} \rangle^2$. We plot these moments in Fig. 1.

Because $\mathcal{L}_k$ is linear, we can represent it as a matrix acting on the space of two-by-two operators. A convenient representation is to write

$$\hat{O} = r_0 \hat{I} + r_1 \sigma_1 + r_2 \sigma_2 + r_3 \sigma_3, \tag{2.34}$$

where $\sigma_{1,2,3} = \sigma_{x,y,z}$ are the usual Pauli matrices. We can then represent $\hat{O}$ by a column vector

$$\hat{O} \equiv \begin{pmatrix} r_0 \\ r_1 \\ r_2 \\ r_3 \end{pmatrix}. \tag{2.35}$$

The action of $\mathcal{L}_k$ on $\hat{O}$ is then given by

$$\mathcal{L}_k\hat{O}\equiv\begin{pmatrix}1 & 0 & 0 & 0\\ 0 & 0 & -(1-p)\sin 2k & \cos 2k\\ 0 & 0 & -(1-p)\cos 2k & -\sin 2k\\ 0 & 1-p & 0 & 0\end{pmatrix}\begin{pmatrix}r_0\\ r_1\\ r_2\\ r_3\end{pmatrix}.$$

(2.36)

Note that since $r_0=\mathrm{Tr}\{\hat{O}\}$, it is unaffected by $\mathcal{L}_k$, which is trace preserving. So the only nontrivial dynamics result from the three-by-three submatrix

$$M_k\equiv\begin{pmatrix}0 & -(1-p)\sin 2k & \cos 2k\\ 0 & -(1-p)\cos 2k & -\sin 2k\\ 1-p & 0 & 0\end{pmatrix}. \quad (2.37)$$

We also need to know the effects of left multiplying and right multiplying by $\hat{Z}$. These are given by the two matrices

$$Z_L\equiv\begin{pmatrix}0 & 0 & 0 & 1\\ 0 & 0 & i & 0\\ 0 & -i & 0 & 0\\ 1 & 0 & 0 & 0\end{pmatrix}, \quad Z_R\equiv\begin{pmatrix}0 & 0 & 0 & 1\\ 0 & 0 & -i & 0\\ 0 & i & 0 & 0\\ 1 & 0 & 0 & 0\end{pmatrix}.$$

(2.38)

Finally, taking the trace picks out the 0 component of the column vector and drops the rest.

Let us take these expressions and apply them to Eq. (2.26) for the first moment. In the integrand, the initial density matrix for the coin is multiplied j times by $\mathcal{L}_k$, then left multi-

plied by $\hat{Z}$, and finally the trace is taken. Given the above expression for Z_L, we see that this is the same as multiplying the three-vector (r_1, r_2, r_3) j times by M_k and then keeping only the r_3 component of the result. This gives us the new expression

$$\langle\hat{x}\rangle_t=-\frac{1}{2\pi}\int dk\begin{pmatrix}0 & 0 & 1\end{pmatrix}\left[\sum_{j=1}^{t}M_k^j\right]\begin{pmatrix}r_1\\ r_2\\ r_3\end{pmatrix}$$

$$=-\frac{1}{2\pi}\int dk(0\ 0\ 1)[(1-M_k)^{-1}(M_k-M_k^{t+1})]$$

$$\times\begin{pmatrix}r_1\\ r_2\\ r_3\end{pmatrix}. \quad (2.39)$$

The eigenvalues of M_k are complicated, but fortunately we do not need to evaluate them. All we need to know is that all of them obey $0<|\lambda|<1$ (where both these inequalities are strict). In the long time limit, therefore, $M_k^{t+1}\rightarrow 0$, and the moment becomes approximately

$$\langle\hat{x}\rangle_t\approx-\frac{1}{2\pi}\int dk(0\ 0\ 1)[(1-M_k)^{-1}M_k]\begin{pmatrix}r_1\\ r_2\\ r_3\end{pmatrix}. \quad (2.40)$$

Note that all t dependence has vanished. Therefore, in the long-time limit, the first moment tends to a constant.

As it happens, the matrix $1-M_k$ is exactly invertible:

$$(1-M_k)^{-1}=\frac{1}{p(2-p)}\begin{pmatrix}1+(1-p)\cos 2k & -(1-p)\sin 2k & (1-p)+\cos 2k\\ -(1-p)\sin 2k & 1-(1-p)\cos 2k & -\sin 2k\\ (1-p)[1+(1-p)\cos 2k] & -(1-p)^2\sin 2k & 1+(1-p)\cos 2k\end{pmatrix}. \quad (2.41)$$

Inserting this and Eqs. (2.37) into (2.40) yields

$$\langle\hat{x}\rangle_t\approx-\frac{1}{2\pi}\int dk\frac{1-p}{p(2-p)}[(1-p)r_3+r_1$$

$$+[r_3+(1-p)r_1]\cos 2k-(1-p)r_2\sin 2k]$$

$$=\frac{1-p}{p(2-p)}[(1-p)r_3+r_1]$$

$$=\frac{1-p}{p(2-p)}[(1-p)(|\alpha|^2-|\beta|^2)+(\alpha^*\beta+\alpha\beta^*)],$$

(2.42)

where the initial state of the coin is $|\Phi_0\rangle=\alpha|R\rangle+\beta|L\rangle$.

In Fig. 2, we compare this result to the results of direct numerical simulation for the initial-state $|\Phi_0\rangle=|R\rangle$. As we can see, the first moment does tend to drift towards a constant value asymptotically. What variation there is a result of statistical error in the Monte Carlo simulation rather than a poor fit.

The second moment is a somewhat more complicated calculation. Let us rewrite the Eq. (2.28) in terms of our four-by-four matrices:
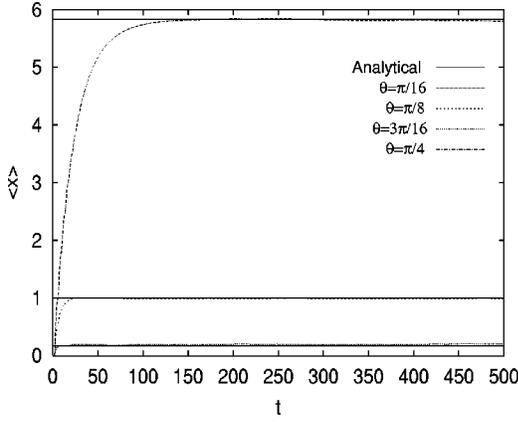
FIG. 2. $\langle \hat{x} \rangle$ vs t for the Hadamard walk on the line with decoherence, for $\theta = \pi/16, \pi/8, 3\pi/16, \pi/4$. For all cases the coin began in the initial state $|R\rangle$. Note that $\langle \hat{x} \rangle$ goes asymptotically to a constant value at long times, which matches our analytical estimate; this drift goes to zero with increasing decoherence, vanishing at $\theta = \pi/4$ (i.e., $p=1$). Note that the irregularities in the broken curves reflect statistical errors in the Monte Carlo calculations.

$$\langle \hat{x}^2 \rangle_t = -\frac{1}{2\pi} \int dk \left[\sum_{j=1}^{t} \sum_{j'=1}^{j} \mathrm{Tr}\{\hat{Z}\mathcal{L}_k^{j-j'}(\hat{Z}\mathcal{L}_k^{j'}|\Phi_0\rangle\langle\Phi_0|)\} \right.$$
$$\left. + \sum_{j=1}^{t} \sum_{j'=1}^{j-1} \mathrm{Tr}\{\hat{Z}\mathcal{L}_k^{j-j'}((\mathcal{L}_k^{j'}|\Phi_0\rangle\langle\Phi_0|)\hat{Z})\} \right]$$

$$= t - \frac{1}{2\pi} \int dk (1\ 0\ 0\ 0)$$

$$\times \left[Z_L \sum_{j=1}^{t} \sum_{j'=1}^{j-1} \mathcal{L}_k^{j-j'}(Z_L+Z_R)\mathcal{L}_k^{j'} \right] \begin{pmatrix} 1 \\ r_1 \\ r_2 \\ r_3 \end{pmatrix}$$

$$= t - \frac{1}{2\pi} \int dk (0\ 0\ 0\ 1)$$

$$\times \left[\sum_{j=1}^{t} \sum_{j'=1}^{j-1} \mathcal{L}_k^{j-j'}(Z_L+Z_R)\mathcal{L}_k^{j'} \right] \begin{pmatrix} 1 \\ r_1 \\ r_2 \\ r_3 \end{pmatrix}. \quad (2.43)$$

The initial t term comes from the $j=j'$ components of Eq. (2.28), where the two factors of $\hat{Z}$ cancel out.

Recall the block-diagonal form Eq. (2.36) of $\mathcal{L}_k$, and note that

$$(Z_L+Z_R) = \begin{pmatrix} 0 & 0 & 0 & 2 \\ 0 & 0 & 0 & 0 \\ 0 & 0 & 0 & 0 \\ 2 & 0 & 0 & 0 \end{pmatrix} \quad (2.44)$$

is extremely sparse. In this case, it makes sense to separate the 0 and 1,2,3 components of the expression:

$$\langle \hat{x}^2 \rangle_t = t - \sum_{j=1}^{t} \sum_{j'=1}^{j-1} \frac{1}{2\pi} \int dk (0\ 0\ 0\ 1)$$

$$\times \left[\mathcal{L}_k^{j-j'}(Z_L+Z_R)\mathcal{L}_k^{j'} \begin{pmatrix} 1 \\ 0 \\ 0 \\ 0 \end{pmatrix} \right.$$

$$\left. + \mathcal{L}_k^{j-j'}(Z_L+Z_R)\mathcal{L}_k^{j'} \begin{pmatrix} 0 \\ r_1 \\ r_2 \\ r_3 \end{pmatrix} \right]. \quad (2.45)$$

We can drop the second term, because it will be canceled in the inner product with (0 0 0 1). This means that $\langle \hat{x}^2 \rangle_t$ has *no dependence* on the initial state! The remaining term becomes

$$\langle \hat{x}^2 \rangle_t = t - \sum_{j=1}^{t} \sum_{j'=1}^{j-1} \frac{1}{2\pi} \int dk (0\ 0\ 0\ 1)\mathcal{L}_k^{j-j'} \begin{pmatrix} 0 \\ 0 \\ 0 \\ 2 \end{pmatrix}$$

$$= t - \frac{1}{2\pi} \int dk (0\ 0\ 1) \left[\sum_{j=1}^{t} \sum_{j'=1}^{j-1} M_k^{j-j'} \right] \begin{pmatrix} 0 \\ 0 \\ 2 \end{pmatrix}$$

$$= t - \frac{1}{2\pi} \int dk (0\ 0\ 1)[t-(1-M_k)^{-1}M_k$$

$$+ (1-M_k)^{-1}M_k^t](1-M_k)^{-1}M_k \begin{pmatrix} 0 \\ 0 \\ 2 \end{pmatrix}. \quad (2.46)$$

In the long-time limit, we can drop the M_k^t terms as negligible. We can thereby substitute the exact expressions (2.37) and (2.41) for the remaining matrices and simplify

$$\langle \hat{x}^2 \rangle_t = t + \frac{1}{2\pi} \int dk \frac{1-p}{p(2-p)} \left[2t(1-p+\cos 2k) \right.$$

$$- \frac{1}{p(2-p)}[4(2-2p+p^2)\cos 2k + (1-p)$$

$$\left. \times (7+\cos 4k)] \right] = t\left(1 + \frac{2(1-p)^2}{p(2-p)}\right) - \frac{7(1-p)^2}{p^2(2-p)^2}. \quad (2.47)$$

Thus, in the case of the decoherent coin the variance will grow linearly with time at long times, just as in the classical
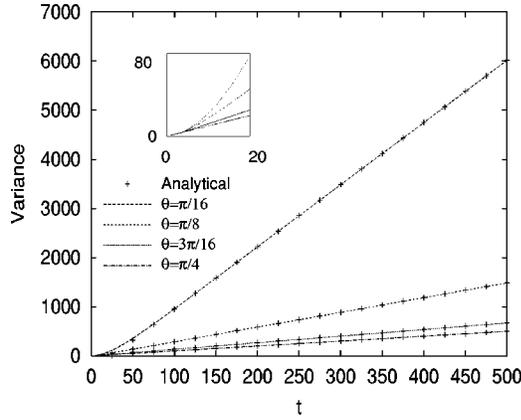
FIG. 3. $\langle \hat{x}^2 \rangle - \langle \hat{x} \rangle^2$ vs t for the quantum random walk with decoherence, for $\theta = \pi/16, \pi/8, 3\pi/16, \pi/4$. For all cases the coin began in the initial state $|R\rangle$. Note that the variance goes asymptotically to a linear growth at long times that matches our analytical estimate; the rate of growth goes to one with increasing decoherence, matching the classical case at $\theta = \pi/4$ (i.e., $p = 1$). The inset shows the time dependence of the variance at short times, where it still exhibits quadratic growth.

case, though the rate of growth will be greater than for the classical random walk. Note that as $p \rightarrow 1$, $\langle \hat{x}^2 \rangle_t \rightarrow t$, which is the classical result.

Because of the dependence of the first moment on the initial condition, the variance will have some residual dependence on the initial condition; but since this is only a constant it is quite unimportant. Upon comparison to the numerical results (see Fig. 3), we see that this analytical expression for the variance matches extremely well.

Since this approximation holds in the long-time limit, it is reasonable to ask how long is a "long time." For weak decoherence ($p \ll 1$), the evolution exhibits the same behavior as the unitary walk for short times, with the second moment growing quadratically in time, and only switches over to linear growth past some critical timescale. This changeover is visible in Fig. 3.

We take the long-time approximation by neglecting the M_k^t term in (2.46). If we examine M_k^2, we see that it can be written as $(1-p)$ multiplying a matrix whose norm is less than one. Therefore, if we want this term to be negligible, then

$$\|M_k^t\| < (1-p)^{t/2} < \epsilon \tag{2.48}$$

for some positive $\epsilon \ll 1$. This implies that

$$p > (2/t)\ln(1/\epsilon) \equiv c/t \tag{2.49}$$

which implies in turn that the second moment of position will grow linearly at $t > c/p$, for a large enough constant c. For $t < c/p$ there will be a transition over to quadratic time dependence. For small p, Eq. (2.47) becomes

$$\langle \hat{x}^2 \rangle_t = t(1 + 1/p) - 7/4p^2. \tag{2.50}$$

III. THE POSITION DISTRIBUTION

As mentioned before, Eq. (2.19) for $p(x,t)$ is difficult to evaluate analytically. It is straightforward, however, to solve this system numerically. Rather than solve for the density-matrix ρ, we instead have used quantum trajectory techniques [25] to do a quantum Monte Carlo simulation, averaging over many runs to find both the distribution itself and its moments.

For the purposes of these simulations, it proved more convenient to use the form Eq. (2.31) for the decoherence process. We have therefore labeled the figures with the appropriate values of the dephasing parameter θ instead of p. In performing the simulations, after each step of the quantum walk we randomly applied either operator $\sqrt{2}\hat{A}_0'$ or $\sqrt{2}\hat{A}_1'$ from Eq. (2.31) to the state, choosing them with equal probability. Because $\sqrt{2}\hat{A}_{0,1}'$ are unitary operators, it was unnecessary to renormalize the state. We then found the mean probability distributions $p(x)$ by averaging over many runs; each distribution plotted in this paper represents an average over 10000 runs of the Monte Carlo program. In Fig. 4 we see how the probability distribution changes as we go to the classical limit of complete decoherence at every step ($\theta = \pi/4$).

As we see from the figure, the presence of decoherence quickly wipes out the most conspicuous signs of interference, the peaks at $\pm t/\sqrt{2}$ and the oscillations in the distribution. A new peak, centered at $t = 0$, makes its appearance, though for weak decoherence it does not have the usual binomial form. However, some residual effects of interference persist up until just short of the classical limit. In particular, the distribution is broadened, with long "tails," and displaced somewhat from the central position. This is reflected in our long-time solution for the variance (2.47), which is higher in the quantum case than the classical except in the limit $p \rightarrow 1$.

In the unitary case, interference effects cause the evolution to "remember" the starting state in a nonintuitive way. As we saw in Fig. 1, if we start the coin in state $|R\rangle$, the system retains a linear drift to the right for all time. If we had instead started in the state $|L\rangle$, the system would have drifted symmetrically to the left. This "memory" also makes the position distribution asymmetric, as we see in Fig. 4(a).

The presence of decoherence eliminates this effect at long times: the system "forgets" the initial conditions after a while. This effect will still persist at short times, however, and produce a tendency for the particle to move repeatedly in the same direction. No doubt this tendency produces the broadening in the position distribution and the significant tails.

IV. CONCLUSIONS

We have examined a possible route from quantum to classical for the quantum random walk: letting the quantum coin undergo decoherence with time. Using the long-time behavior of the position moments as a qualitative marker of classicality, we see that even very weak decoherence changes the growth of the variance from a quadratic to a linear function
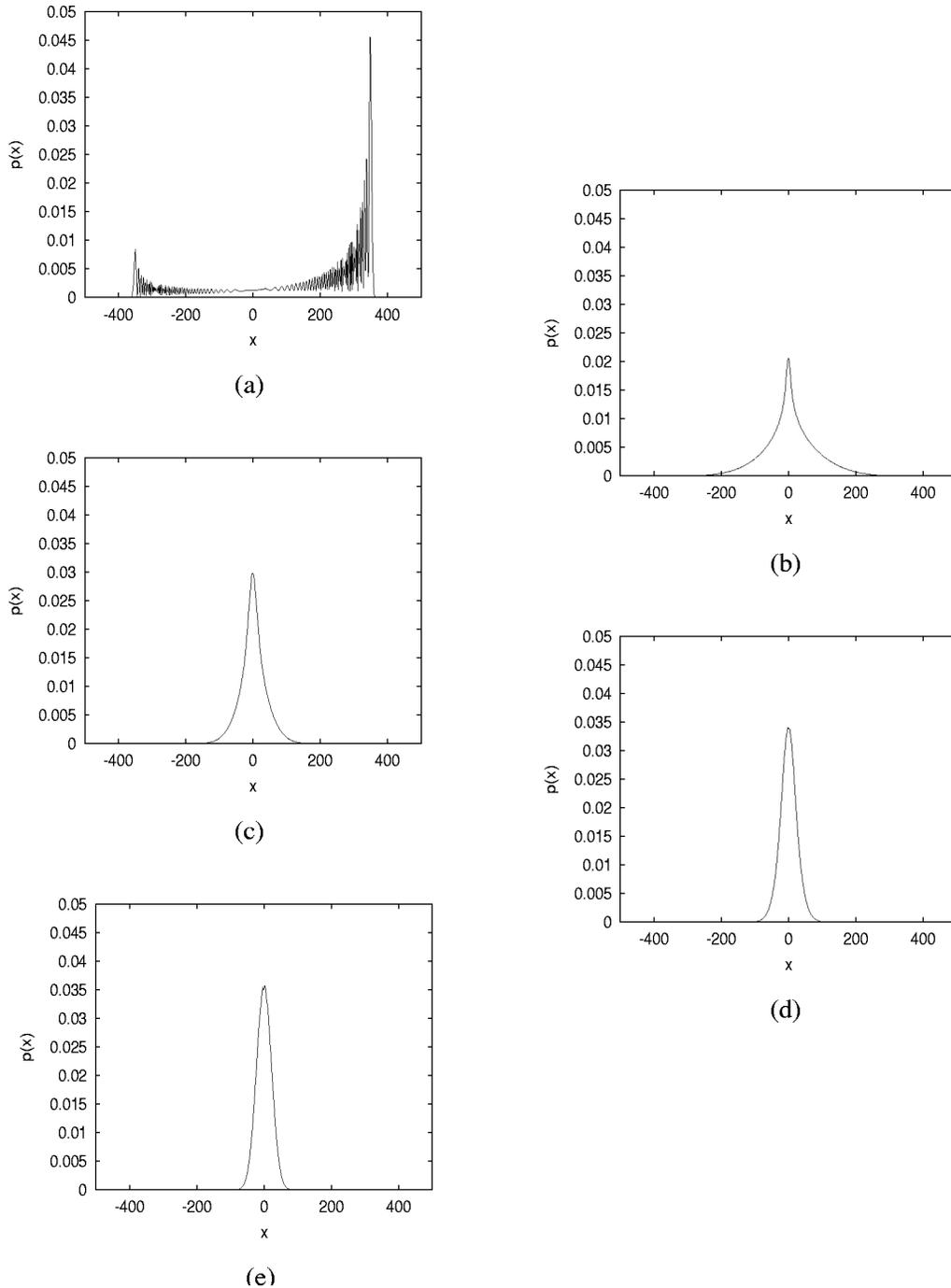
FIG. 4. The probability distributions $p(x,t)$ at $t=500$ for the quantum random walk with decoherence: (a) $\theta=0$ (unitary case), (b) $\theta=\pi/16$, (c) $\theta=\pi/8$, (d) $\theta=3\pi/16$, (e) $\theta=\pi/4$ (classical case). A central peak appears when decoherence is included, which becomes increasingly dominant; however, the peak is broadened compared to the classical case, with nontrivial tails, which disappear only in the classical limit, when $p(x,t)$ goes over to the binomial distribution.

of time. Since the usual classical random walk has a linear growth of the variance, in a particular sense we can claim that the decoherent walk is indeed classical.

This situation is quite different from the quantum random walk with multiple coins [24]; for that system, quadratic growth remained except in the limit of a new coin for every step. One might reasonably claim that the multicoin system remains "quantum" even in the limit of very large numbers of coins, while the decoherent system remains "classical" even in the limit of very weak noise.

In spite of this, some effects of interference are important even in the presence of decoherence. In particular, the variance grows more rapidly in the quantum than the classical case. This may reflect a tendency for the particle to be "biased" in one direction for short times, while interference effects enable it to "remember" its starting state. This is

consistent with the position distributions, which are broader than the classical binomial distribution, and have nontrivial tails.

In the long time limit, the time dependence of the moments becomes tractable because the evolution superoperator has only one eigenvalue of modulus 1. All other components decay away exponentially with time. It is interesting to speculate whether a decoherence process with several modulus 1 eigenvalues might continue to exhibit quantum behavior. This is probably possible, at least for higher-dimensional coins.

We should emphasize that the system we have studied in this paper has decoherence only in the coin degree of freedom; any effects of decoherence on the particle are indirect. It might be arguably natural to include decoherence in the particle position as well. Such systems have been studied numerically, and exhibit interesting effects of their own [20,22,26].

[1] E. Farhi and S. Gutmann, Phys. Rev. A **58**, 915 (1998).

[2] A.M. Childs, E. Farhi, and S. Gutmann, Quantum Inf. Proc. **1**, 35 (2002).

[3] A.M. Childs, R. Cleve, E. Deotto, E. Farhi, S. Gutmann, and D.A. Spielman, e-print quant-ph/0209131.

[4] Y. Aharonov, L. Davidovich, and N. Zagury, Phys. Rev. A **48**, 1687 (1993).

[5] D.A. Meyer, J. Stat. Phys. **85**, 551 (1996); e-print quant-ph/9604003.

[6] A. Nayak and A. Vishwanath, e-print quant-ph/0010117.

[7] D. Aharonov, A. Ambainis, J. Kempe, and U. Vazirani, in *Proceedings of ACM Symposium on Theory of Computation (STOC'01), July 2001* (Association for Computing Machinery, New York, 2001), pp. 50–59; e-print quant-ph/0012090.

[8] A. Ambainis, E. Bach, A. Nayak, A. Vishwanath, and J. Watrous, in *Proceedings of ACM Symposium on Theory of Computation (STOC'01), July 2001* (Ref. [7]), pp. 37–49.

[9] D.A. Meyer and H. Blumer, e-print quant-ph/0110028.

[10] C. Moore and A. Russell, e-print quant-ph/0104137.

[11] T. MacKay, S. Bartlett, L. Stephenson, and B. Sanders, J. Phys. A **35**, 2745 (2002); e-print quant-ph/0108004.

[12] J. Kempe, e-print quant-ph/0205083.

[13] N. Konno, T. Namiki, and T. Soshi, e-print quant-ph/0205065.

[14] N. Konno, e-print quant-ph/0206053.

[15] N. Konno, e-print quant-ph/0206103.

[16] B.C. Travaglione and G.J. Milburn, Phys. Rev. A **65**, 032310 (2002).

[17] J. Du, H. Li, X. Xu, J. Wu, X. Zhou, and R. Han, e-print quant-ph/0203120.

[18] T. Yamasaki, H. Kobayashi, and H. Imai, e-print quant-ph/0205045.

[19] B.C. Sanders, S.D. Bartlett, B. Tregenna, and P.L. Knight, e-print quant-ph/0207028.

[20] W. Dür, R. Raussendorf, V. Kendon, and H.-J. Briegel, e-print quant-ph/0207137.

[21] E. Bach, S. Coppersmith, M.P. Goldschen, R. Joynt, and J. Watrous, e-print quant-ph/0207008.

[22] V. Kendon and B. Tregenna, e-print quant-ph/0209005.

[23] T. Brun, H. Carteret, and A. Ambainis, e-print quant-ph/0208195.

[24] T. Brun, H. Carteret, and A. Ambainis, e-print quant-ph/0210161.

[25] H.J. Carmichael, *An Open Systems Approach to Quantum Optics* (Springer-Verlag, Berlin, 1993), and references therein, among others.

[26] V. Kendon and B. Tregenna, e-print quant-ph/0210047.